Korean J. Chem. Eng., **31**(5), 807-811 (2014)
DOI: 10.1007/s11814-013-0290-6

pISSN: 0256-1115
eISSN: 1975-7220

Effects of ultrasonic radiation on induction period and nucleation kinetics of sodium sulfate

Guisheng Zeng*,,†, Hui Li*, Shenglian Luo*, Xianyong Wang*, and Junhong Chen****

*Key Laboratory of Jiangxi Province for Persistent Pollutants Control and Resources Recycle, School of Environment and Chemical Engineering, Nanchang Hangkong University, Nanchang 330063, China
**Department of Mechanical Engineering, University of Wisconsin-Milwaukee, Milwaukee, Wisconsin 53211, USA
(*Received 17 June 2013 • accepted 23 December 2013*)

Abstract–The effects of ultrasound on crystal nucleation and particle size distribution of sodium sulfate were investigated via determining the induction period and particle size. Crystal nucleation parameters and equations for primary nucleation were calculated. The experimental results show that the induction time decreases under the ultrasound irradiation, therefore, we can get a shorter induction period at a higher supersaturation level. Based on these observations, the growth mechanism of sodium sulfate is continuous growth because the value of the surface entropy factor *f* is smaller than 3. The induction period was observed shorter and particle size was smaller when the ultrasonic radiation time increased. Crystal growth improved with the longer crystallization time.

Keywords: Sodium Sulfate, Crystallization, Ultrasound, Primary Nucleation, Particle Size

INTRODUCTION

Crystallization is a common method to purify and separate substances out of solutions, and also is performed from melt in addition to solutions, which is used in many chemical and pharmaceutical industries [1]. It is a very important unit operation, resulting in the separation of solid phase from its original liquid phase system. It industrially accounts for over 70% of solids produced in chemical and pharmaceutical processes. Especially, mixed suspension mixed product removal mixed suspension (MSMPR) crystallizer is widely used in researches, providing a standard crystallization technique. According to laboratory research, this method may be a suitable crystallizer to produce crystal products as an industrial crystallization method. The crystal products must have high purity and high yield as well as desired crystal size and size distribution.

The crystallization process consists of three basic steps: supersaturation of solution, formation of nuclei, and growth of crystals. The growth rate of crystals depends on the level of supersaturation as the driving force for crystal growth. It is used on a large scale in glass, synthetic fiber, paper, and other industries. Marliacy et al. [2] studied the thermodynamics of crystallization of sodium sulfate decahydrate solution in H_2O-NaCl-Na_2SO_4. Vavouraki and Koutsoukos [3] investigated the kinetics of crystal growth of mirabilite ($Na_2SO_4 \cdot 10H_2O$) in aqueous supersaturated solutions. Steiger and Asmussen [4] examined the phase diagram of Na_2SO_4-H_2O and observed the generation of stress. Rodriguez-Navarro et al. [5] investigated the crystallization of sodium sulfate as a method to examine concrete and other building materials. Genkinger and Putnis [6] revealed crystallization of sodium sulfate solutions through evaporation under controlled conditions. Marzal and Scherer [7] investigated the crystallization of sodium sulfate salts in Cordova Cream and Indiana limestone.

In addition to ultrasound irradiation as the dominant method to initiate and control crystallization processes, there are some other ways to control crystallization processes. Ultrasound has been applied to crystallizing systems, offering a significant potential for modifying and improving both processes and products [8-12]. Nucleation control using ultrasonic irradiation has been studied and shown to be an effective technique for obtaining better crystals [13-17]. It is a powerful tool to induce crystal nucleation and to improve product properties. Ultrasound is known to influence the crystallization system in several ways, such as reduction in induction time for crystallization and narrowing down crystal size distribution. The true chemical effects of ultrasound are attributed to the implosive collapse of microbubbles that are formed during rarefaction, or negative pressure period of sound waves. The implosive collapse of microbubbles—typically referred to as cavitation—also results in a variety of mechanical effects [18]. The process of formation and collapse of microbubbles is shown in Fig. 1. Narducci et al. [19] revealed the steady state particle size distribution under continuous ultrasonic

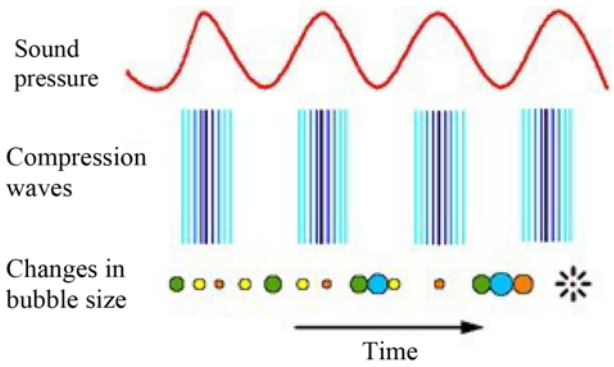

Fig. 1. Process of formation and collapse of microbubbles.

†To whom correspondence should be addressed.
E-mail: zengguisheng@hotmail.com

irradiation. Sayan et al. [20] studied the average particle size of crystals under power ultrasound. Harzali et al. [21] investigated the induction time of $ZnSO_4 \cdot 7H_2O$ crystallization as a function of supersaturation in ultrasonic conditions. All these investigations provide some information about the influence of ultrasound on the crystal properties. However, the main nucleation mechanism under ultrasound irradiation is not completely known yet. Moreover, the crystal growth mechanism of sodium sulfate and the nucleation equation have not been reported. To the best of our knowledge, there has not been any published work dealing with the induction period and particle size under various ultrasonic conditions, such as time, power, and frequency.

The purpose of this work is to study the influence of ultrasonic wave on the induction period and particle size of anhydrous sodium sulfate crystals during cooling crystallization process. Compared to other works, the influence of ultrasonication on crystallization process is optimized and the form of the first crystal nucleus is observed with the help of a self-design laser detection system. Growth mechanism and the nucleation process of sodium sulfate are investigated by classical nucleation theory. Induction time (t_{ind}), surface entropy factor (f), surface energy (γ), nucleate rate (B^0) and crystal size distribution (CSD) are studied with different ultrasound time and power.

THEORY

In this paper, we identify the crystal nucleation and growth mechanism of sodium sulfate through measuring the induction time. According to classical nucleation theory (CNT) [22-24], the nucleation rate B of sphaerocrystals can be expressed as

$$B = A\exp\left(-\frac{16\gamma^3 V_m^2}{3\upsilon^2 k^3 T^3 \ln^2 S}\right) \quad (1)$$

where B is the nucleation rate, V_m is the volume of molecule, k is the Boltzmann constant, T is the absolute temperature, S is the supersaturation ratio, γ is the crystal-solution interfacial tension, and ν is the moles of ions per mole of the solute.

The induction time has an inverse ratio relationship with nucleation rate:

$$t_{ind}^{-1} \propto B \quad (2)$$

Thus, the relationship between induction time and supersaturation can be expressed as

$$\ln t_{ind} = K + \frac{16\gamma^3 V_m}{3\upsilon^2 k^3 T^3 \ln^2 S} \quad (3)$$

From Eq. (3), it is known that a straight line for plot of $\ln t_{ind}$ against $1/\ln^2 S$ can be obtained with a slope given in Eq. (4)

$$\alpha = \frac{16\gamma^3 V_m}{3\upsilon^2 k^3 T^3} \quad (4)$$

Then, the interfacial tension can be calculated as

$$\gamma = \left(\frac{3\alpha\upsilon^2 k^3 T^3}{16 V_m^2}\right)^{1/3} \quad (5)$$

The value of *f* can be obtained from the interfacial tension using Eq. (6)

$$f = \frac{4V_m^{2/3}\gamma}{kT} \quad (6)$$

Surface entropy factor *f* is an important parameter to determine the roughness degree of the crystal surface. A larger value of *f* indicates that the crystal surface is smoother and crystal growth becomes more difficult. Therefore, *f* is always used to identify the mechanism of crystal growth. When the *f* value is smaller than 3, continuous growth will occur and when *f* is between 3 and 5, nucleation and growth of crystals are expected to occur. When *f* is greater than 5, spiral growth happens.

A cavitation bubble is produced in liquid with ultrasound radiation. The bubbles are nucleated, grown, closed, and collapsed under the alternating vibration between phases in compression and expansion conditions. The cavitation bubbles produce high temperature and pressure during the collapse process of bubbles. Moreover, high speed fluid impulse friction and intense ultrasonic irradiation and violent chemical reaction are also generated during the process. All these functions lead to crystallization with the assistance of ultrasound waves.

EXPERIMENTAL

1. Materials

Sodium sulfate was prepared with purity of larger than 99.9 wt%. Deionized water was used to make saturated solution.

2. Apparatus

A laser method (SGN-3) was applied to measure the induction time of sodium sulfate. A schematic diagram of the experimental apparatus is shown in Fig. 2. Experiments were performed in a 200 ml double-jacket glass crystallizer. Solutions with different supersaturation ratio (S) of sodium sulfate at 29 °C were prepared on the basis of the solubility data published [3]. The supersaturation ratio S is defined as the ratio of the concentration in the bulk to the solubility at a certain temperature. The solution was heated to 34 °C, 5 °C above the saturation temperature, to ensure complete dissolution of the solute and then was fed into the crystallizer. Supersaturation was achieved via cooling crystallization. Moreover, it was lower than the saturation temperature of the solution in the same

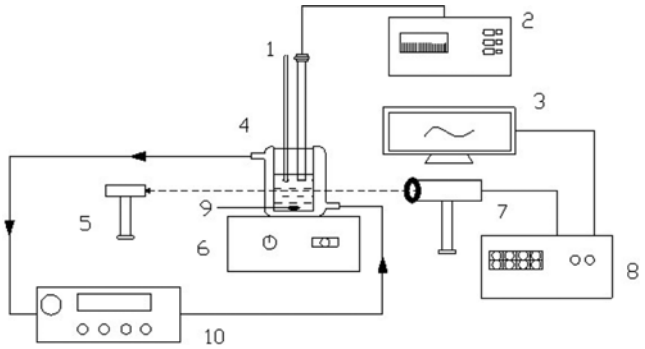

Fig. 2. Schematic diagram of ultrasonic velocity equipment.

1. Thermometer
2. Ultrasound generator
3. Recorder
4. Jacket crystallizer
5. Laser generator
6. Magnetic stirrers
7. Laser power receiver
8. Photoelectric converter
9. Magneton
10. Super-thermostat water bath

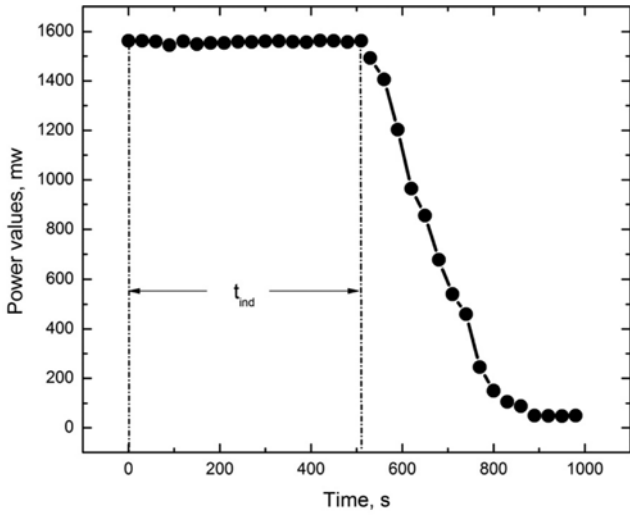

Fig. 3. Image of induction time (t_{ind}) in cooling crystallization of sodium sulfate.

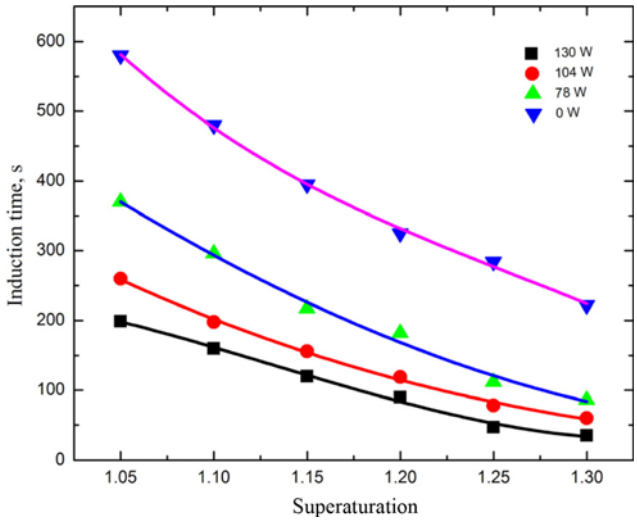

Fig. 4. Effects of supersaturation on induction period under silent and ultrasound conditions.

conditions. A thermostatic water bath (model SYC-15B) was used for precise temperature control in the crystallizer. An ultrasonic power supplier (Sonics VCX 130 PB) was used to produce various ultrasonic powers. The resonance frequency of the equipment was 20 KHz and the equipment had 130W HF output. Ultrasonic energy was introduced into the system via an ultrasonic horn. An ultrasonic probe, made of titanium alloy Ti-6Al-4V with diameter of 3 mm, was directly immersed into the solution. The system was run for the periods of residence times in order to attain a steady state in the crystallizer. The examined induction periods are presented in Fig. 3. Then, crystals were separated from the mother liquor with vacuum filtration system. Crystals were dried before being used for further studies. Particle size was determined with LA-950 laser particle analyzer (Horiba Company, Japan). The morphology of crystals was examined by scanning electron microscopy technique (SEM, S-3500N, Hitachi Company, Japan).

RESULTS AND DISCUSSION

1. Effect of Supersaturation on Induction Period

The induction times with various ultrasonic power values and without ultrasound irradiation are presented in Fig. 4. Two phenomena were observed. First, the induction periods dramatically decreased with increasing ultrasonic irradiation, compared with the one without ultrasonic irradiation. Moreover, induction time decreased when the ultrasonic output at each supersaturation increased. The second observation was that the induction periods increased with decreasing of supersaturation. The SEM micrographs of crystals with and without ultrasonic power (Fig. 5) clearly indicate that clear crystals with larger particle size were obtained in the absence of ultrasonic radiation. Whereas, with increasing the ultrasonic power, the particle size of crystal decreased. The shapes of crystals were observed approximately spherical.

According to classical nucleation theory, a linear relationship between ln t_{ind} and $1/\ln^2 S$ was fitted, as presented in Fig. 6. Two different straight lines were obtained for this system. The slope at higher supersaturation was observed larger than that at lower supersaturation. This phenomenon implies two different crystallization mechanisms. At high supersaturation, homogeneous nucleation is dominant mechanism as there is enough driving force in the salt solution. However, at low supersaturation, heterogeneous nucleation is the main mechanism and can occur more often than homogeneous nucle-

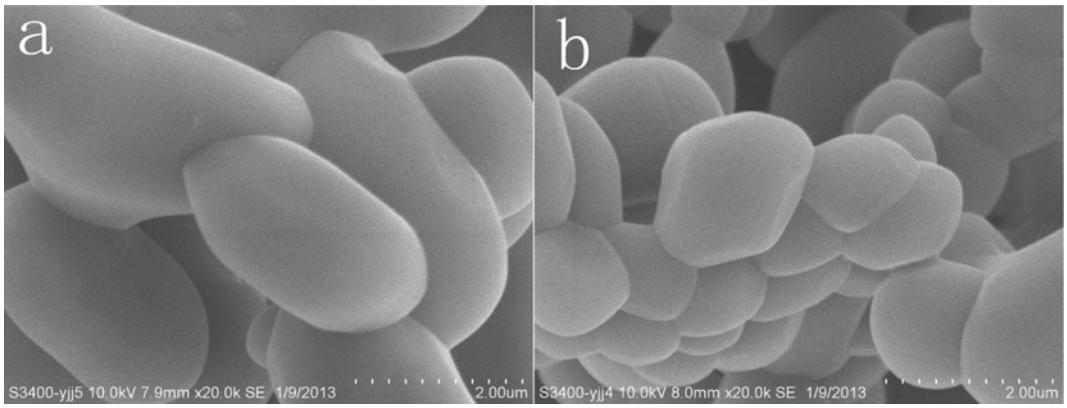

Fig. 5. The SEM of sodium sulfate in ultrasound (130 W) and without ultrasound: (a) without ultrasound; (b) 130 W ultrasound power.

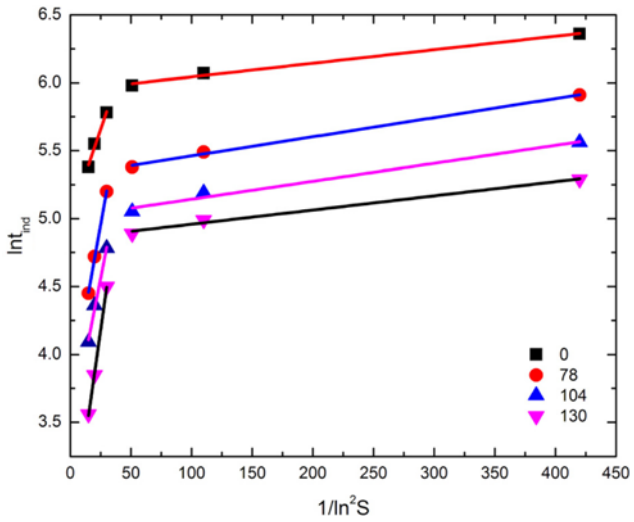

Fig. 6. Plot of ln t_{ind} against $1/\ln^2 S$ for sodium sulfate at various power ultrasound values.

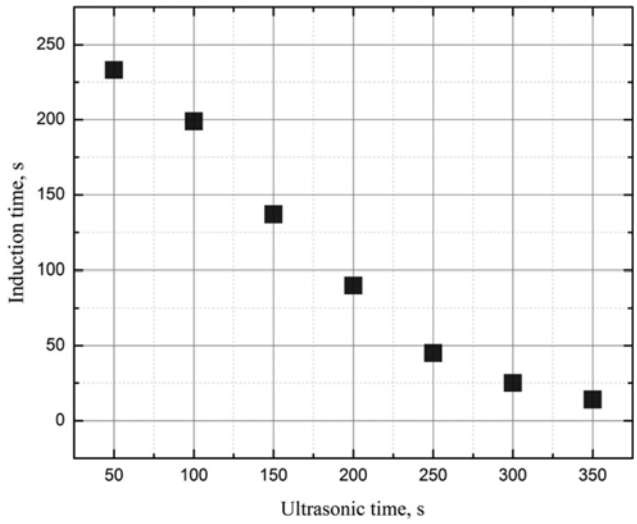

Fig. 7. Effect of ultrasonic irradiation time on induction time.

Table 1. The fitting parameters for $\ln t_{ind}$ against $1/\ln^2 S$ and the surface entropy factor *f*

Power (W)	Nucleation	α	R^2	γ (N/m^2)	*f*
0	Homogeneous	0.0261	0.9786	7.05×10^{-3}	0.2538
	Heterogeneous	0.0010	0.9875	2.38×10^{-3}	0.0860
78	Homogeneous	0.0497	0.9982	8.73×10^{-3}	0.3143
	Heterogeneous	0.0014	0.9953	2.66×10^{-3}	0.0958
104	Homogeneous	0.0454	0.9915	8.48×10^{-3}	0.3053
	Heterogeneous	0.0013	0.9716	2.61×10^{-3}	0.0940
130	Homogeneous	0.0630	0.9985	9.45×10^{-3}	0.3402
	Heterogeneous	0.0015	0.9827	7.05×10^{-3}	0.0868

ation. Heterogeneous nucleation is usually induced by foreign particles, such as dusts, decreasing the energy required for nucleation of new crystals. The fitting parameters for ln t_{ind} against $1/\ln^2 S$ and the surface entropy factor *f* were calculated using Eq. (6) and the values are listed in Table 1. From the results, we can conclude that the growth mechanism of sodium sulfate is continuous growth because the *f* value is smaller than 3.

2. Crystal Growth and Effect of Ultrasound Time on Induction Period

Rodriguez-Navarroa et al. investigated the ESEM micrographs of the anhydrous sodium sulfate at different RH and temperatures without a detailed investigation of the crystal growth mechanism [5]. When crystallization proceeded, the crystal size increased. The results for induction time measured at various ultrasonic irradiation times are shown in Fig. 7. The induction time decreased when the ultrasonic time increased. To better understand the mechanism of ultrasonication, we studied the produced sodium sulfate crystals with different ultrasound time. The particle size of the crystal was obtained from SEM images (Fig. 8) and Malvern laser particle size analyzer (Fig. 9). Figs. 8 and 9 indicate smaller crystals were obtained at longer period of ultrasonic time, while larger crystals were obtained in shorter periods. This phenomenon can be explained because ultrasound can break the tiny crystals down more quickly, then the crystals are dissolved to the solution, which results in the growth of bigger crystals with the increase of saturation. It obeys the Ostwald ripening mechanism and longer ultrasound time makes the Ostwald phenomenon more obvious [25]. The mean size of crystals decreases from 1.80±0.25 to 1.28±0.17 μm, as the ultrasound time increases from 30s to 150 s.

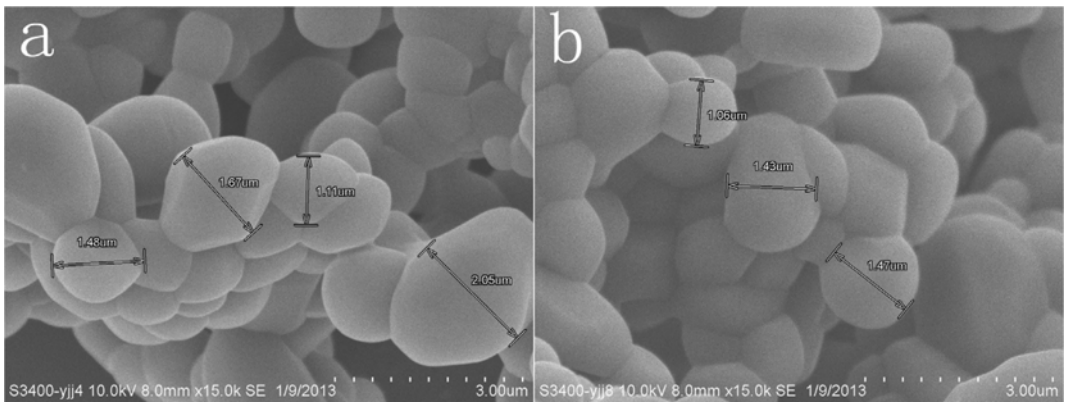

Fig. 8. The SEM of sodium sulfate in different ultrasonic time (a) 30 s (b) 150 s.

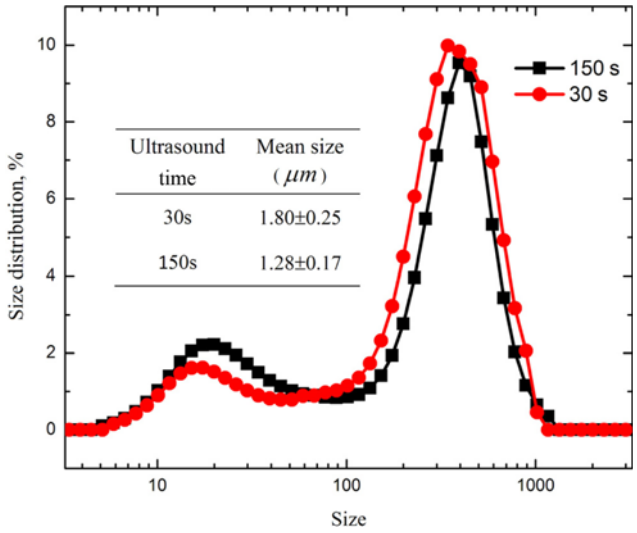

Fig. 9. The CSD of sodium sulfate in different ultrasonic time (30 s and150 s).

CONCLUSIONS

The influence of ultrasonic irradiation on the induction period and nucleation kinetics of sodium sulfate was studied. The results show that the induction time decreases with increasing supersaturation level and ultrasonic power. By increasing the ultrasonic power, the induction period becomes shorter and the particle size of crystal decreases. According to classical nucleation theory, the relationship between ln t_{ind} and $1/\ln^2 S$ was studied to determine the crystallization parameters. From the results and calculated nucleation parameters, we can conclude that the growth mechanism of sodium sulfate is a continuous process as the *f* value was smaller than 3. With respect to effects of ultrasonic irradiation time on the induction period and particle size, the induction period was shorter and the particle size was observed smaller with increasing the ultrasonic time because of the microbubbles of ultrasound. Crystal growth was improved at longer crystallization time.

ACKNOWLEDGEMENTS

This work was financially supported by the National Natural Science Foundation of China (51266011), the National High Technology Research and Development Program of China (2010AA065204), and the Jiangxi Provincial Department of Education (GJJ13505). The authors appreciate the assistance of Dr. Saeed Doroudiani in editing the manuscript.

REFERENCES

1. M. Kurotani, M. Etsuko, E. Satomi and H. Izumi, *J. Cryst. Growth*, **311**, 2714 (2009).
2. P. Marliacy, R. Solimando, M. Bouroukba and L. Schuffenecker, *Thermochim. Acta*, **344**, 85 (2000).
3. A. I. Vavouraki and P. G. Koutsoukos, *J. Cryst. Growth*, **338**, 189 (2012).
4. M. Steiger and S. Asmussen, *Geochim. Cosmochim. Acta*, **72**, 4291 (2008).
5. C. Rodriguez-Navarro, E. Doehne and E. Sebastian, *Cem. Concr. Res.*, **30**, 1527 (2000).
6. S. Genkinger and A. Putnis, *Environ. Geol.*, **52**, 329 (2007).
7. R. M. E. Marzal and G. W. Scherer, *Environ. Geol.*, **56**, 605 (2008).
8. A. Kordylla, S. Koch, F. Tumakaka and G. Schembecker, *J. Cryst. Growth*, **310**, 4177 (2008).
9. G. Ruecroft, D. Hipkiss, T. Ly, N. Maxted and P. W. Cains, *Org. Process Res. Dev.*, **9**, 923 (2005).
10. H. Harzali, F. Baillon, O. Louisnard, F. Espitalier and A. Mgaidi, *Chem. Eng. J.*, **195**, 332 (2012).
11. K. Wohlgemuth, F. Ruether and G. Schembecker, *Chem. Eng. Sci.*, **65**, 1016 (2010).
12. O. Narducci, A. G. Jones and E. Kougoulos, *Chem. Eng. Sci.*, **66**, 1069 (2011).
13. H. Li, H. Li, Z. Guo and Y. Liu, *Ultrason. Sonochem.*, **13**, 359 (2006).
14. E. Miyasaka, M. Takai, H. Hidaka, Y. Kakimoto and I. Hirasawa, *Ultrason. Sonochem.*, **13**, 308 (2006).
15. H. Li, J. Wang, Y. Bao, Z. Guo and M. Zhang, *J. Cryst. Growth*, **247**, 192 (2003).
16. Z. Guo, A. G. Jones and N. Li, *Chem. Eng. Sci.*, **61**, 1617 (2006).
17. K. Wohlgemuth, A. Kordylla, F. Ruether and G. Schembecker, *Chem. Eng. Sci.*, **64**, 4155 (2009).
18. L. H. Thompson and L. K. Doraiswamy, *Ind. Eng. Chem. Res.*, **38**, 1215 (1999).
19. O. Narducci, A. G. Jones and E. Kougoulos, *Cryst. Growth Des.*, **11**, 1742 (2011).
20. P. Sayan, S. T. Sargut and B. Kiran, *Ultrason. Sonochem.*, **18**, 795 (2011).
21. H. Harzali, F. Espitalier, O. Louisnard and A. Mgaidi, *Phys. Procedia*, **3**, 965 (2010).
22. M. C. Weinberg, W. H. Poisl and L. Granasy, *C. R. Chim.*, **5**, 765 (2002).
23. G. F. Neilson and M. C. Weinberg, *J. Non-Cryst. Solids*, **34**, 137 (1979).
24. F. Bakhtar, J. B. Young, A. J. White and D. A. Simpson, *J. Mech. Eng. Sci.*, **219**, 1315 (2005).
25. K. V. Saban, T. Jini and G. Varghese, *Cryst. Res. Technol.*, **40**, 748 (2005).